

Band-Structure Analysis from Electro-Reflectance Studies

B. O. SERAPHIN* AND N. BOTTKA

Michelson Laboratory, China Lake, California

(Received 10 August 1965; revised manuscript received 3 January 1966)

This paper provides the analytical tools for an interpretation of the electro-reflectance effect in semiconductors, which is observed as a change in the reflectance in the presence of an electric field at approximately the photon energies of interband transitions. Previously only applicable to ϵ_2 at an M_0 -type absorption edge, the theory of Franz and Keldysh is expanded for the most general case of field-induced changes of both ϵ_1 and ϵ_2 at both M_0 - and M_1 -type edges. Every member of this group of four components displays a highly individual line shape and symmetry character, facilitating the recognition of basic patterns in the experimentally observed structure. By comparing such structure with the calculated line shapes, an assignment to interband transitions of a certain type and at certain photon energies will be suggested. The coefficients which determine the fractional contributions of $\Delta\epsilon_1$ and $\Delta\epsilon_2$ to the change in reflectance in different spectral regions are calculated for Ge, Si, and GaAs. The analysis is applied to the 3.4-eV region in Si, and satisfactory agreement with experiment is obtained by placing a parabolic M_0 -type edge at 3.33 eV and a saddle-point M_1 -type edge at 3.41 eV. The calculation produces a shift of the effect with increasing average field toward shorter wavelengths for the parabolic and toward longer wavelengths for the saddle-point edge. This is in agreement with experimental observations for Si and GaAs and confirms a valuable experimental criterion which discriminates between the two different types of interband transitions.

INTRODUCTION

THIS paper analyzes an effect which is observed as a change in the reflectance of a semiconductor induced by an electric field perpendicular to the reflecting surface.¹ Since the reflectance responds to the electric field in a pronounced structure of peaks at approximately the photon energies of interband transitions, the effect will add to the information that band-structure analysis extracts from optical studies on semiconductors. The derivative nature of the effect enhances the structure considerably in comparison to ordinary reflectance studies, providing much higher resolution and sensitivity.² Moreover, the effect gives information which makes the assignment of structure in the reflectance to the correlated interband transitions less ambiguous by establishing experimental criteria which discriminate among the different types of these interband transitions.³ This paper provides the analytical tools for such an interpretation of the electro-reflectance effect with respect to band structure analysis.

Early studies of the fundamental absorption edge in germanium suggested that the change in the reflectance was caused by a modulation of the electric field in the surface potential barrier of the reflecting surface and that the underlying phenomena was a Franz-Keldysh effect observed in reflection rather than in transmission. With this assumption, the calculation produced satisfactory agreement with the experimental results, but

only after two difficulties were overcome: (1) The Franz-Keldysh theory had to be employed in full, using numerical evaluations rather than asymptotic expansions of the Airy function; and (2) since the Franz-Keldysh theory calculates the field-induced change in the imaginary part ϵ_2 of the dielectric constant, while the reflectance in this spectral region, however, is predominantly determined by the real part ϵ_1 , the experimental quantity $\Delta R/R$ had to be related to theory through Kramers-Kronig integrals.⁴

Later experimental work proved that the electro-reflectance effect was present not only at the fundamental absorption edge, but at higher interband edges as well.^{2,5} This confronted the analysis with two problems which had to be solved before the interpretation could be extended into the region above the fundamental edge: First, the reflectance response is composed not only of contributions from ϵ_1 as in the case of the fundamental edge, but also of contributions from ϵ_2 , and the proportions of ϵ_1 and ϵ_2 are different in different parts of the spectrum. Secondly, the higher interband edges to which the observed reflectance structure correlates may not be of the same type as the fundamental edge, which necessarily must be a parabolic edge (M_0 type). Since the effect of the electric field on the density-of-state function may be entirely different at a saddle-point edge of the type M_1 , no predictions could be made until this effect was calculated in Phillips' duality theorem.⁶

The following study expands the analysis in both respects and presents a framework of calculations into which, in principle, the structure of the reflectance response to the electric field should fit for every part of

* Present address: U. S. Office of Naval Research, Keyser House, 429 Oxford St., London, W.1, England.

¹ B. O. Seraphin, in *Proceedings of the International Conference on the Physics of Semiconductors, Paris, 1964* (Dunod Cie., Paris, 1964), p. 165; B. O. Seraphin, R. B. Hess, and N. Bottka, *J. Appl. Phys.* **36**, 2242 (1965).

² B. O. Seraphin and R. B. Hess, *Phys. Rev. Letters* **14**, 138 (1965).

³ B. O. Seraphin, *Proc. Phys. Soc. (London)* **87**, 239 (1966); *J. Appl. Phys.* **37**, 721 (1966).

⁴ B. O. Seraphin and N. Bottka, *Phys. Rev.* **139**, A560 (1965).

⁵ B. O. Seraphin, *Phys. Rev.* **140**, A1716 (1965).

⁶ J. C. Phillips, *Proceedings of the International School of Physics "Enrico Fermi," 1966* [Nuovo Cimento Suppl. (to be published)].

the spectrum and for both types of interband transitions. In Sec. I is recapitulated the formalism which describes the influence of an electric field on ϵ_1 and ϵ_2 in the neighborhood of a critical point of the parabolic type. Normalized $\Delta\epsilon_1$ and $\Delta\epsilon_2$, which will later serve as the basic building blocks for the analysis and which can be carried through the necessary mathematics in a linear form, are defined. Section II describes the transformation which is used to calculate the influence of the electric field at a saddle-point edge from the same effect at a parabolic edge. More realistic expressions are obtained in Sec. III by exposing the calculated absorption edges to lifetime-broadening.

At this point of the analysis, the changes in ϵ_1 as well as in ϵ_2 , induced by an electric field around both types of edges, are available. Section IV now investigates the extent to which $\Delta\epsilon_1$ and $\Delta\epsilon_2$ contribute to the reflectance response $\Delta R/R$ in different parts of the spectrum. For three different materials, Ge, Si, and GaAs, the fractional coefficients α and β which determine this contribution are calculated. Section V discusses, from a general point of view, what can be learned from the symmetry properties and the sign of the components $\Delta\epsilon_1$ and $\Delta\epsilon_2$, as well as their superposition in $\Delta R/R$ for spectral regions, in which either one or the other of the fractional coefficients α and β predominate or in which they both contribute equally. Using the 3.4-eV region in *n*-type Si as an example, it is demonstrated how the assignment of structure to correlated transitions can be guided by these properties. On the basis of the previous calculations, the conclusion is inevitable that the structure in this region correlates to a parabolic edge preceding a saddle-point edge by about 0.1 eV, a conclusion which could be supported previously only by rather circumstantial evidence. Finally, Sec. VI calculates how a given peak of the reflectance response shifts with an increase in the average electric field around which the ac voltage modulates, with the result that structure related to parabolic edges shifts opposite to structure related to saddle-point edges. This provides an experimental criterion for the assignment of structure to either type of transition. An example demonstrates that the direction and magnitude of the calculated field shift agrees with experimental observations on GaAs,³ where such an "anti-Franz-Keldysh" shift was actually reported for the structure observed at 2.9 and 3.1 eV, correlating it unambiguously to a saddle-point edge.

I. NORMALIZED FRANZ-KELDYSH EFFECT AT A PARABOLIC EDGE

In the weak-field approximation, sufficient for the purpose of this study, Tharmalingam and Callaway⁷ find for the absorption coefficient $\alpha(\omega, F)$ in the presence of

an electric field F the following expression, which holds throughout the region of the fundamental absorption edge:

$$\alpha(\omega, F) = \frac{R}{\omega} \theta_F^{1/2} \left[\left| \frac{d \text{Ai}(\beta)}{d\beta} \right|^2 - \beta |\text{Ai}(\beta)|^2 \right], \quad (1)$$

where $R = (2e^2 C_0^2 / \hbar c n m^2) (2\mu/\hbar)^{3/2}$; $\theta_F^3 = e^2 F^2 / 2\mu\hbar$ and $\beta = (\omega_1 - \omega) / \theta_F$. $\text{Ai}(\beta)$ is the Airy function, defined by

$$\text{Ai}(\beta) = \frac{1}{\sqrt{\pi}} \int_0^\infty \cos\left(\frac{1}{3}u^3 + u\beta\right) du. \quad (2)$$

C_0 is a constant involving the matrix elements between the periodic parts of the Bloch states at the band edges, in addition to material parameters and fundamental constants. $\hbar\omega_1$ is the energy of the band gap, and μ is the reduced mass of the electron-hole pair for this transition. e , m , \hbar , and c have their usual meanings.

Applying the relations between the optical constants n and α and the imaginary part ϵ_2 of the complex dielectric constant, it follows that

$$\epsilon_2(\omega, F) = (nc/\omega)\alpha(\omega, F) \quad (3)$$

and therefore

$$\epsilon_2(\omega, F) = (B/\omega^2)\theta_F^{1/2}\{\text{Airy}\}, \quad (4)$$

where $B = (2e^2 C_0^2 / \hbar m^2) (2\mu/\hbar)^{3/2}$ does not contain the frequency except for a slight dependence through the matrix elements. $\{\text{Airy}\}$ is an abbreviation for the expression inside the brackets of Eq. (1), which depends only upon the difference of the frequency with respect to the edge ω_1 .

For $F \rightarrow 0$, Eq. (4) goes over into the familiar expression for the absorption due to direct allowed transitions above a parabolic edge ($\omega > \omega_1$),⁸

$$\epsilon_2(\omega, 0) = 0.3187 \times (B/\omega^2) (\omega - \omega_1)^{1/2}, \quad (5)$$

and gives $\epsilon_2 \rightarrow 0$ as $F \rightarrow 0$ below the edge ($\omega < \omega_1$).

It was shown in a previous paper⁴ in what manner the constant B in front of an expression of the type of Eq. (5) can be used as a free parameter in order to fit the field-free case as closely as possible to the experimentally observed absorption curve. Rather than calculating the absorption coefficient in the presence of an electric field from first principles, this adjustment process makes the electric field act as an operator on an experimentally observed curve. In this analysis, the constant B will be used in an even wider sense, representing the "strength" of the transition.

Multiplying ϵ_2 by ω^2/B results in an expression which is independent of the actual location of the edge and of its strength. A normalized parabolic edge (PAR) at $\hbar\omega_1$ is therefore defined as one for which the following

⁷ K. Tharmalingam, Phys. Rev. **130**, 2204 (1963); J. Callaway, *ibid.* **130**, 549 (1963); **134**, A998 (1964).

⁸ J. Bardeen, F. J. Blatt, and L. H. Hall, *Photoconductivity Conference* (John Wiley & Sons, Inc., New York, 1956), p. 146.

relation holds

$$[\text{Norm}(\epsilon_2)_{\text{PAR}}] = (\omega^2/B)\epsilon_2 = 0.3187(\omega - \omega_1)^{1/2}, \quad (\omega > \omega_1). \quad (6)$$

Multiplying Eqs. (4) and (5) by ω^2/B , and subtracting, gives the change in the imaginary part of the dielectric constant in normalized form at such an edge

$$\begin{aligned} [\text{Norm}(\Delta\epsilon_2)_{\text{PAR}}] &= \theta_F^{1/2}\{\text{Airy}\} - 0.3187(\omega - \omega_1)^{1/2}, \\ & \quad (\omega > \omega_1) \\ &= \theta_F^{1/2}\{\text{Airy}\}. \quad (\omega < \omega_1). \end{aligned} \quad (7)$$

The field-induced change in ϵ_2 causes a related change in ϵ_1 , which is determined by the Kramers-Kronig dispersion relation⁹

$$\Delta\epsilon_1(\omega, F) = -\frac{2}{\pi} \int_0^\infty \frac{\omega' \Delta\epsilon_2}{\omega'^2 - \omega^2} d\omega'. \quad (8)$$

It is not immediately obvious from Eq. (8) that $\Delta\epsilon_1$ can be written in the same normalized form as $\Delta\epsilon_2$. No closed analytical expression could be found which made $(\omega^2/B)\Delta\epsilon_1$ strictly independent of $\hbar\omega_1$. Numerical computation of Eq. (8) for several values of $\hbar\omega_1$ in the interval from 0 to 5 eV showed, however, that $(\omega^2/B)\Delta\epsilon_1$ does not change more than 1% in this interval.

The normalized change in the real part of the dielectric constant is therefore defined as

$$[\text{Norm}(\Delta\epsilon_1)_{\text{PAR}}] = (\omega^2/B)\Delta\epsilon_1. \quad (9)$$

Plots of the numerical values of $[\text{Norm}(\Delta\epsilon_1)_{\text{PAR}}]$ and

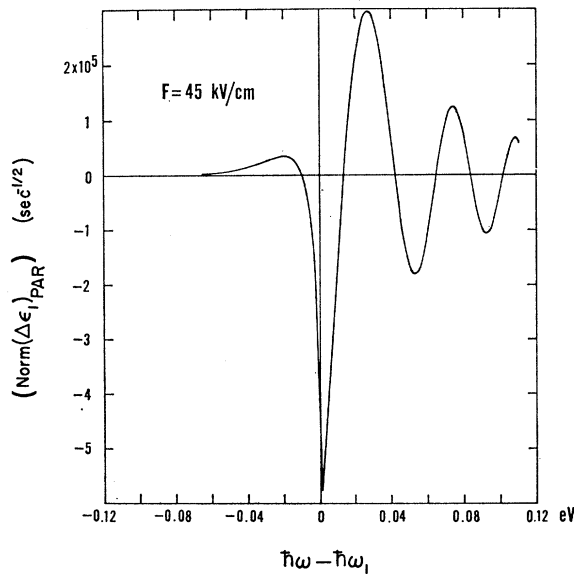


FIG. 1. The normalized change of the real part ϵ_1 of the dielectric constant, as induced at a parabolic edge by an electric field of 45 kV/cm.

⁹ F. Stern, *Solid State Physics* (Academic Press Inc., New York, 1963), Vol. 15, p. 327; *Phys. Rev.* 133, A1653 (1964).

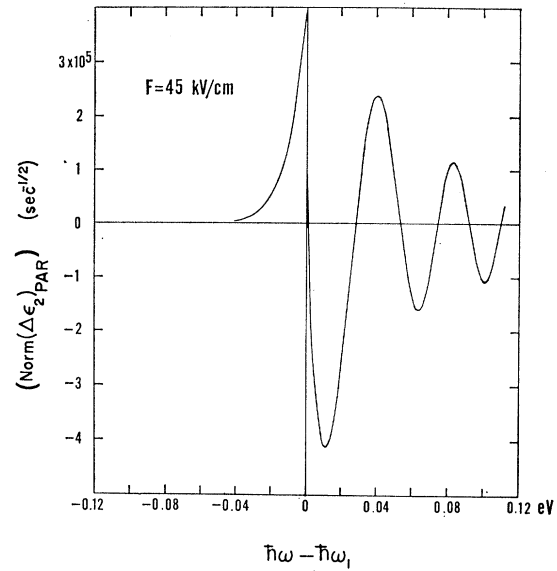


FIG. 2. The normalized change of the imaginary part ϵ_2 of the dielectric constant, as induced at a parabolic edge by an electric field of 45 kV/cm.

$[\text{Norm}(\Delta\epsilon_2)_{\text{PAR}}]$ are shown in Figs. 1 and 2 as functions of the distance $\hbar(\omega - \omega_1)$ from the parabolic edge. An electric field of 45 kV/cm is representative for the surface potential barrier of a semiconductor. The details of the numerical calculations of Eqs. (7) and (9) were described in a previous paper.⁴

In closing this section the importance of this normalization should be emphasized. The fact that $\Delta\epsilon_1$ as well as $\Delta\epsilon_2$ can be separated into one part which depends only upon the relative distance from the edge $\hbar(\omega - \omega_1)$, multiplied by the square of the frequency, will facilitate the final analysis. The experimentally observed quantity

$$(\Delta R/R) = (B/\omega^2)[\alpha(\omega) \times \text{Norm}(\Delta\epsilon_1) + \beta(\omega) \times \text{Norm}(\Delta\epsilon_2)] \quad (10)$$

can now be discussed mainly in terms of the spectral dependence of the fractional coefficients α and β , since most observed structure has only a width of the order of 0.1 eV, so that ω^2 can be considered constant for one group of peaks. The appearance of an observed group of peaks as to sign and multiplicity can be reproduced by arranging the normalized values of $\Delta\epsilon_1$ and $\Delta\epsilon_2$ on the energy scale until the experimental result is matched as closely as possible, considering the fractional coefficients α and β only. The final size of the calculated structure can be adjusted in two ways: either by determining the "strength" of the transition from a match between Eq. (5) and an experimental absorption curve, or, in cases where the related absorption edge cannot be distinguished with sufficient contrast, by matching the observed $\Delta R/R$ as to the magnitude. If the modulating electric field is known with sufficient

accuracy, this second process should permit conclusions to be drawn as to the magnitude of the parameters contained in B , i.e., reduced mass and matrix elements.

II. NORMALIZED FRANZ-KELDYSH EFFECT AT A SADDLE-POINT EDGE

Since the Franz-Keldysh effect was previously observed in transmission only, the experiment was restricted to the fundamental absorption edge.¹⁰ Representing a minimum in the band separation in k space, this edge is necessarily of the parabolic type and no need existed for an expansion of the theory to other types of transitions. The observation of the Franz-Keldysh effect in reflection on interband edges above the fundamental edge changed this situation. First the theory, in order to be expanded to saddle-point edges, must take into account that the effect could now be produced at critical points located on interband-energy surfaces of less than cubic symmetry. Consequently the effect must be expected to vary with the angle between the electric field and the principal axis of the saddle-point surface. Polarization of the light and orientation of the reflecting surface will be of importance.¹¹ Secondly, the square-root singularities in the joint density-of-state function, which lead to an expression for ϵ_2 of the type of Eq. (5) in the case of a parabolic edge, now have the form

$$\epsilon_2(\omega, 0)_{\text{SP}} = A - 0.3187(B/\omega^2)(\omega_1 - \omega)^{1/2}, \quad (\omega < \omega_1) \quad (11)$$

for a saddle-point edge. In order to establish the effect of an electric field F on such a nondegenerate M_1 -type saddle-point edge, Phillips proved the following duality theorem for the case that F is parallel to the principal axis of the isoenergetic saddle-point cone: The change in ϵ_2 at a saddle-point edge is obtained from the corresponding change at a parabolic edge by reversing the signs of $(\omega - \omega_1)$ and $\Delta\epsilon_2$.⁶ The theorem is illustrated in a qualitative form in Fig. 3.

It follows from the transformation properties of the theorem that the field-induced change in ϵ_2 is given in a normalized form at a saddle-point edge by

$$\begin{aligned} [\text{Norm}(\Delta\epsilon_2)_{\text{SP}}] &= 0.3187(\omega_1 - \omega)^{1/2} - \theta F^{1/2} \{ \text{Airy} \}, & (\omega < \omega_1) \\ &= -\theta F^{1/2} \{ \text{Airy} \}, & (\omega > \omega_1). \end{aligned} \quad (12)$$

Notice that $\Delta\epsilon_2$ is independent of the "background" term A on either side of the edge. The normalized form can be carried through the Kramers-Kronig integral, giving the normalized change $[\text{Norm}(\Delta\epsilon_1)_{\text{SP}}] = (\omega^2/B)\Delta\epsilon_1$. No separate diagrams for $[\text{Norm}(\Delta\epsilon_1)_{\text{SP}}]$

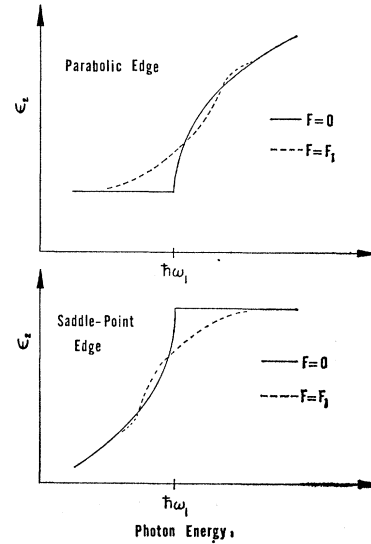


FIG. 3. The field-induced change in ϵ_2 at a parabolic and a saddle-point edge, according to Phillips duality theorem.

or $[\text{Norm}(\Delta\epsilon_2)_{\text{SP}}]$ are given, since they can be derived from Figs. 1 and 2 by simple transformations.

Notice, however, that this transformation is entirely different for the real part of the dielectric constant compared to the imaginary part. The change in ϵ_2 , for which the duality theorem applies, transforms like a reflection at the origin: $(\omega - \omega_1) \rightarrow (\omega_1 - \omega)$ and $\Delta\epsilon_2 \rightarrow -\Delta\epsilon_2$. This is *not* true for the change in ϵ_1 , since the "weighting function" $(\omega'^2 - \omega^2)^{-1}$ contained in the Kramers-Kronig integral causes $\Delta\epsilon_1$ to transform as reflection about ω_1 only, so that the duality theorem must read in this case: $(\omega - \omega_1) \rightarrow (\omega_1 - \omega)$ and $\Delta\epsilon_2 \rightarrow \Delta\epsilon_2$. This can easily be seen for a point ω in the neighborhood of the edge: A value $\Delta\epsilon_2$ to the right of the edge is transformed into its negative value at an equal distance to the left of the edge. While previously weighted by a negative $(\omega'^2 - \omega^2)^{-1}$, the negative value after transformation is now weighted by a positive $(\omega'^2 - \omega^2)^{-1}$, so that the sign of the product is unchanged. Upon integration over ω' , the above difference in the transformation properties of $\Delta\epsilon_1$ and $\Delta\epsilon_2$ is demonstrated.

III. THE EFFECT OF LIFETIME BROADENING

The strong oscillations of $\Delta\epsilon_1$ and $\Delta\epsilon_2$ behind the edge as shown in Figs. 1 and 2 are probably not a realistic description of the situation. Lifetime broadening due to interaction with phonons leads to an intrinsic level width of more than 0.05 eV in the region of the edge, so that the prospects for resolving these Stark splittings are not favorable. The experiment supports this view since only one high-energy satellite is observed, and this is presumably just the vestige of the Stark oscillations.¹

In order to obtain a more realistic picture of the

¹⁰ T. S. Moss, J. Appl. Phys. 32, 2136 (1961); D. Williams, Phys. Rev. 126, 442 (1962); M. Chester and P. H. Wendland, Phys. Rev. Letters 13, 193 (1964); A. Frova and P. Handler, *ibid.* 14, 178 (1965); L. M. Lambert, Phys. Rev. 138, A1569 (1965).

¹¹ J. C. Phillips and B. O. Seraphin, Phys. Rev. Letters 15, 107 (1965).

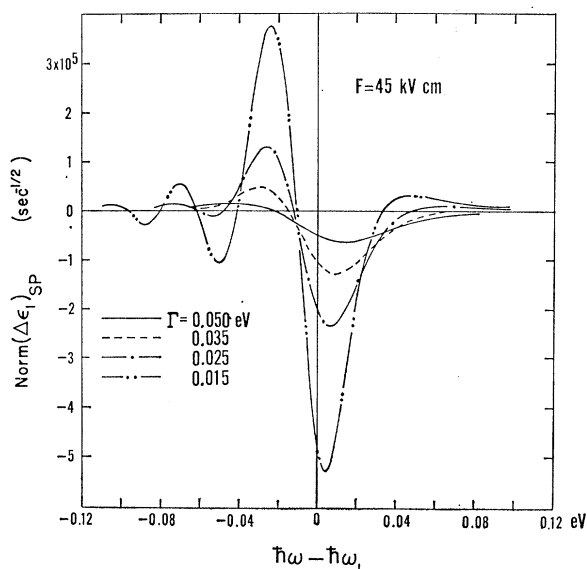


FIG. 4. The normalized change in ϵ_1 at a saddle-point edge, which is exposed to lifetime broadening with different Lorentzian parameters Γ .

absorption process, lifetime broadening is introduced using the convolution

$$\epsilon_2(\omega, F)_{LB} = \int_0^{\infty} \frac{\Gamma \epsilon_2(\omega', F)}{(\omega - \omega')^2 + \Gamma^2} d\omega'. \quad (13)$$

The field-induced change $\Delta\epsilon_2(\omega, F)_{LB}$ is calculated by convoluting $\epsilon_2(\omega, 0)$ and $\epsilon_2(\omega, F)$ separately and then forming the difference. $\Delta\epsilon_1(\omega, F)_{LB}$ is calculated by integrating over $\Delta\epsilon_2(\omega, F)_{LB}$ according to Eq. (8).

The numerical values for both quantities are plotted in Figs. 4 and 5 for different values of the Lorentzian

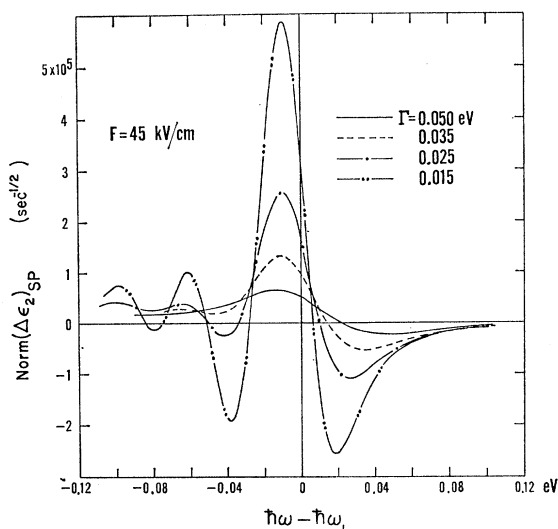


FIG. 5. The normalized change in ϵ_2 at a saddle-point edge, which is exposed to lifetime broadening with different Lorentzian parameters Γ .

broadening parameter Γ and, for a fixed $\Gamma=0.035$ eV, in Figs. 6 and 7 for different values of the electric field. Except for the elimination of the parentheses, no separate nomenclature is introduced for the lifetime-broadened values, which are used exclusively from now on through the rest of the paper, with the value $\Gamma=0.035$ eV. This is close to $2kT$ at 200°K , at which temperature most of the significant measurements were taken. Notice that introduction of lifetime broadening has the desired effect of damping the oscillations above the edge and rounding off the spike whose sharpness is an artificial product of the calculations.

For small broadening $\Gamma=0.015$ eV, comparison of Fig. 1 with Fig. 4 and of Fig. 2 with Fig. 5 reflects the

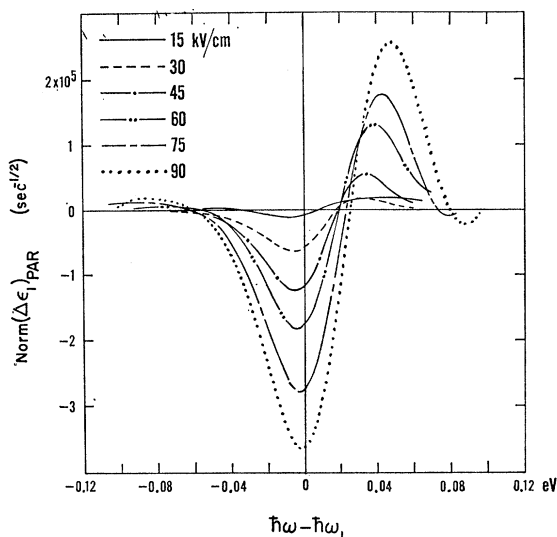


FIG. 6. The normalized change in ϵ_1 at a parabolic edge, lifetime broadened with $\Gamma=0.035$ eV, for different electric fields.

difference of the transformation for $\Delta\epsilon_1$ and $\Delta\epsilon_2$: Fig. 1 transforms into Fig. 4 (except for the broadening) by reflection at the ordinate. Figure 2 goes over into Fig. 5 by a 180-deg rotation around the origin.

It should be pointed out, that the narrow range of suitable Γ values represents a result of physical significance. The order of magnitude estimate of Γ , as obtained from ordinary reflectance measurements, is 0.1 eV. The high resolution of the electro-reflectance effect in conjunction with these calculations permits the deduction of the Lorentzian broadening parameter with much greater precision. $\Gamma=0.015$ eV must be considered too small because the strong oscillations still existing in the calculation for this value are not observed in the experiment. $\Gamma=0.050$ eV, on the other hand, suppresses the effect to an extent that the constant B in Eq. (5) cannot be matched in ϵ_2 . Hence it is reasonable to conclude $\Gamma=0.030\pm 0.010$ eV, a value of considerably greater precision than any previously

obtained from experiments with less resolution. The implication is that it is now possible to measure the Lorentzian lifetime-broadening parameter as a function of energy and temperature using the electro-reflectance technique.

IV. THE FRACTIONAL COEFFICIENTS α AND β

The analysis has now progressed to the point where the effect of the electric field on the real as well as on the imaginary part of the dielectric constant can be calculated. The field-induced changes in ϵ_1 and ϵ_2 depend only on the relative distance from either a parabolic or a saddle-point edge, so that the edge can be placed at any point on the energy scale. Strength of the transition and actual photon energy are added to the normalized form as multiplicative factors.

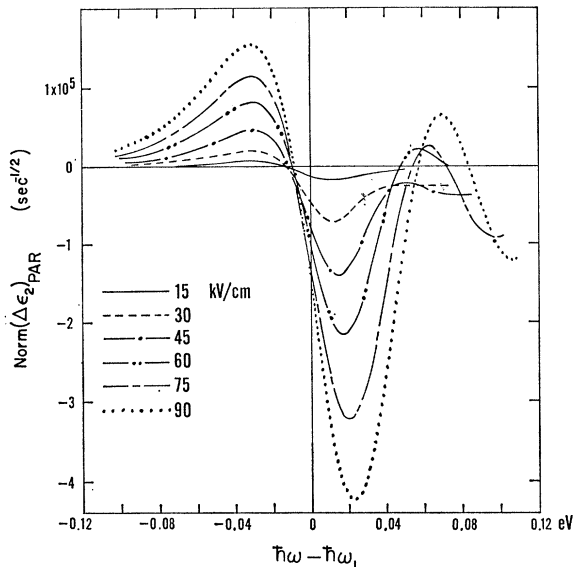


FIG. 7. The normalized change in ϵ_2 at a parabolic edge, lifetime broadened with $\Gamma=0.035$ eV, for different electric fields.

Proceeding further from such a knowledge of $\Delta\epsilon_1$ and $\Delta\epsilon_2$ as functions of the modulating electric field, the analysis must now evaluate to what extent these two functions contribute to the change in reflectance $\Delta R/R$. Differentiating Fresnel's formula, expressed in ϵ_1 and ϵ_2 , gives

$$\Delta R/R = \alpha(\epsilon_1, \epsilon_2)\Delta\epsilon_1 + \beta(\epsilon_1, \epsilon_2)\Delta\epsilon_2, \quad (14)$$

where

$$\alpha \equiv C_1 [(\epsilon_1 - 1)A_+ + \epsilon_2 A_-], \quad (15)$$

$$\beta \equiv C_2 [(\epsilon_1 - 1)/A_+ - \epsilon_2/A_-], \quad (16)$$

with

$$A_{\pm} \equiv \pm \frac{\sqrt{2} [(\epsilon_1^2 + \epsilon_2^2)^{1/2} \pm \epsilon_1]^{1/2}}{(\epsilon_1^2 + \epsilon_2^2)^{1/2}},$$

$$C_1 \equiv [(\epsilon_1 - 1)^2 + \epsilon_2^2]^{-1};$$

$$C_2 \equiv 2\epsilon_2 / [(\epsilon_1 - 1)^2 + \epsilon_2^2](\epsilon_1^2 + \epsilon_2^2).$$

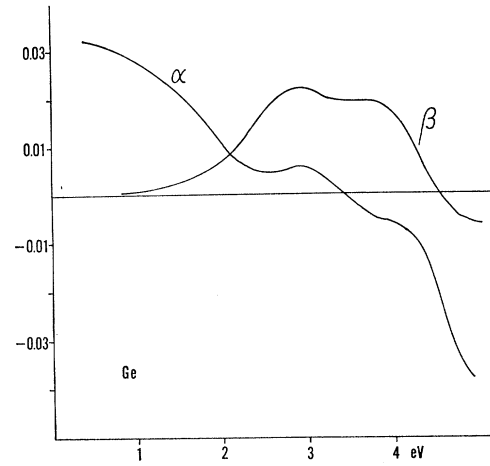


FIG. 8. The fractional coefficients α and β in Eq. (14) for germanium, after Ref. 12.

The fractional coefficients α and β are functions of photon energy, and their sign and relative magnitude determine the result of the analysis in the different spectral regions. Figures 8 through 10 plot these coefficients for Ge, Si, and GaAs, as calculated from experimental values of the optical constants.¹² The three diagrams are very similar: A low-energy region, which contains the fundamental absorption edge, is dominated by α . The α dominance in this region makes it difficult to understand the Franz-Keldysh effect in reflection without applying the Kramers-Kronig dispersion relation. Rising β and falling α produce a crossover, which in all three materials is located near a region of pronounced structure in the reflectance. α goes through

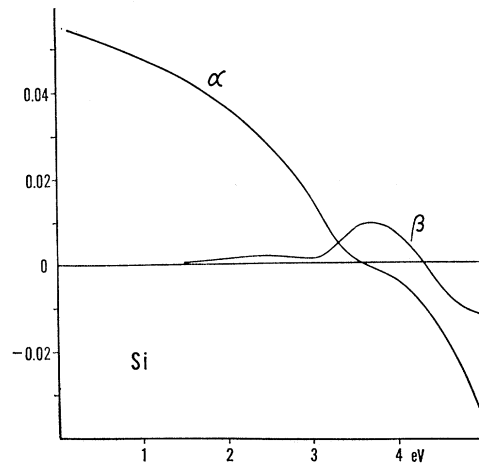


FIG. 9. The fractional coefficients α and β in Eq. (14) for silicon, after Ref. 12.

¹² H. R. Philipp and E. A. Taft, Phys. Rev. 120, 37 (1960); H. Ehrenreich and H. R. Philipp, in Proceedings of the International Conference on the Physics of Semiconductors, Exeter, 1962 (The Institute of Physics and The Physical Society, London, 1962), p. 367.

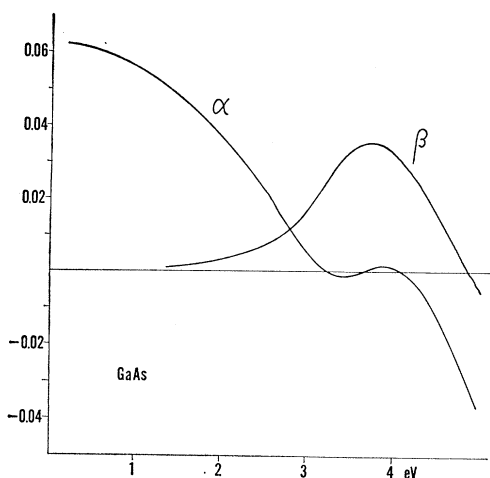


FIG. 10. The fractional coefficients α and β in Eq. (14) for gallium arsenide, after Ref. 12.

zero and changes sign in the region where β is strongest; β then also goes through zero. The change of sign in β is again a region of structure in the reflectance of all three materials.¹³

V. ANALYSIS OF THE 3.4-eV REGION IN SILICON

Figures 4 through 7 show the four basic elements of the analysis: the electric-field-induced changes in ϵ_1 and ϵ_2 on a parabolic as well as on a saddle-point edge. The different transformations which derive them from ϵ_2 at a parabolic edge give them a different appearance with respect to general symmetry, ratio of the peak height, and location relative to the edge. At both types of edges, $\Delta\epsilon_1$ is characterized by two peaks of opposite sign, the larger peak being negative and located close to the edge. The sequence, however, reads down-up at the parabolic edge and up-down at the saddle point. $\Delta\epsilon_2$ shows a strong center peak, surrounded by satellites on either side. The center peak is positive and below the edge in the parabolic, and negative and above the edge in the saddle-point case.

If structure is observed at a given photon energy, the signs and relative sizes of α and β must first be determined. This decides the fractions of the contribution of $\Delta\epsilon_1$ and $\Delta\epsilon_2$ to the reflectance response $\Delta R/R$ at this photon energy. After this determination, both types of edges can be tried with this mixture, moving them through the region of the structure. The best fit with the experiment determines the final selection.

This adjustment process is demonstrated for the 3.4-eV region in *n*-type Si. As shown by the dashed line in Fig. 11, a threefold structure of one positive and two

negative peaks is experimentally observed.¹⁴ At 3.33 eV Fig. 9 shows that α and β are of about equal size. The reflectance response consists therefore of approximately equal contributions from $\Delta\epsilon_1$ and $\Delta\epsilon_2$. For a saddle-point edge, this ratio produces an up-down sequence of approximately equal peak size, which is not observed. Better agreement is obtained for the parabolic edge, which gives a strong negative peak above the edge.

Leaving the first negative peak and proceeding to 3.4 eV, α decreases quickly and yields completely to the growing β at 3.5 eV. The remaining part of the structure is therefore β dominated. The experiment can be reproduced with the up-down structure of a saddle-point $\Delta\epsilon_2$, placed at 3.41 eV, with the small admixture of $\Delta\epsilon_1$ emphasizing this line shape.

The solid curve in Fig. 11 was computed by superimposing all four components, taking the spectral dependence of α and β into account point by point:

$$\frac{\Delta R}{R} = [\alpha(\omega)\Delta\epsilon_1(\omega) + \beta(\omega)\Delta\epsilon_2(\omega)]^{3.33 \text{ eV PAR}} + [\alpha(\omega)\Delta\epsilon_1(\omega) + \beta(\omega)\Delta\epsilon_2(\omega)]^{3.41 \text{ eV SP}} \quad (17)$$

The Lorentzian broadening parameter Γ is 0.035 eV. The details for the experimental curve are reported in separate papers.^{5,14}

Since no other arrangement of edges reproduces the observed structure as well, the conclusion seems inevitable that this structure is correlated to a parabolic edge at 3.33 eV and a saddle-point edge at 3.41 eV, in agreement with previous assignment.^{11,15} As derived from Poisson's equation in the surface potential barrier, the modulating field is not constant in the region of the optical absorption, so hence no conclusions can be drawn from the magnitude of B which matches the size of the response in Eq. (10). The same B , however, roughly matches Eq. (5) assuming the value for ϵ_2 of Si at 3.4 eV.¹²

The positive peak is produced automatically by the calculations as a satellite structure, though it has been classified from experiments by its response to temperature and field as of excitonic origin.

VI. ANTI-FRANZ-KELDYSH EFFECT AT SADDLE-POINT EDGES

This final section demonstrates how the transformation properties of the duality theorem provide, in the form of an anti-Franz-Keldysh effect, criteria for the assignment of structure to transitions even more

¹⁴ B. O. Seraphin and N. Bottka, Phys. Rev. Letters **15**, 104 (1965).

¹⁵ H. Ehrenreich, H. Philipp, and J. C. Phillips, Phys. Rev. Letters **8**, 59 (1962); J. C. Phillips, *Solid State Physics*, edited by F. Seitz and D. Turnbull (Academic Press Inc., New York, 1966), Vol. 18; D. Brust, Phys. Rev. **134**, A1337 (1964); M. L. Cohen and J. C. Phillips, *ibid.* **139**, A912 (1965); G. W. Gobeli and E. O. Kane, Phys. Rev. Letters **15**, 142 (1965).

¹³ M. Cardona, J. Appl. Phys. **32**, 2151 (1961); T. M. Donovan, E. J. Ashley, and H. E. Bennett, J. Opt. Soc. Am. **53**, 1403 (1963); U. Gerhardt, Phys. Letters **9**, 118 (1964).

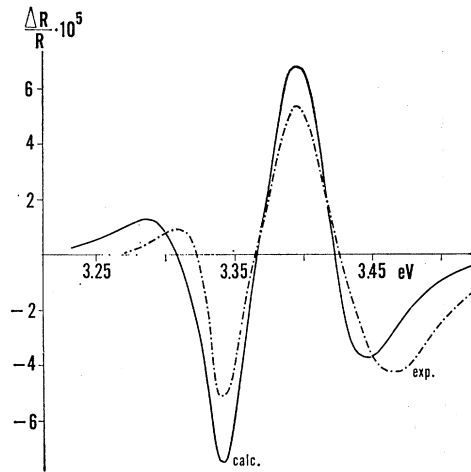


FIG. 11. Comparison between the reflectance response, as experimentally observed in *n*-type silicon, and the response calculated for a parabolic edge at 3.33 eV and a saddle-point edge at 3.41 eV.

powerful than the adjustment procedure described in the previous section.

It is a consequence of the $X \rightarrow -X$ part of this transformation that systematic shifts of peaks with the electric field, for instance, go in one direction for a saddle-point edge and in the opposite direction for a parabolic edge. Notice that this inversion holds for $\Delta\epsilon_1$ as well as for $\Delta\epsilon_2$, since $X \rightarrow -X$ is common to both of them. Conclusions as to the inversion of the sign of a peak must be drawn cautiously, however, since the inversion $Y \rightarrow -Y$ is valid only for $\Delta\epsilon_2$ and occurs therefore only for regions of β predominance.

Figure 12 shows such a shift for the arrangement of edges described in the previous section. It is assumed here that a constant ac field of 15 kV/cm modulates around different values of a superimposed dc bias, producing a voltage swing as indicated in the figure. The response of the structure to the change in dc bias is different in different parts: The negative peak, resulting from the parabolic edge, moves toward higher photon energies with increasing dc bias, while the two peaks correlated to the saddle-point edge shift in the opposite direction. This is in agreement with experimental observations on *n*-type Si, as reported elsewhere.⁵

Turning the argument around, the shift of an experimentally observed structure with dc bias can be used to guide the assignment. Caution must be exercised in this, however, since the satellites of a dispersive structure show a more complicated pattern, as described and calculated in Ref. 4. On the other hand, generalizing observations made in detail by simultaneous observation of electrical and optical field effect in Ge, the shift pattern (long-wavelength satellite: constant or red shift; center peak: slight blue shift; short-wavelength satellite: strong blue shift) can be used to distinguish satellites from center peaks by the relation of their field shifts.

This shift pattern, which is a consequence of the model of the surface potential barrier rather than being specific for one material, was used in the assignment of structure in GaAs.³ The circles in Fig. 13 are taken from this paper. They plot the position of four main peaks in the two groups E_0 and E_1 as a function of the dc bias around which the ac field of constant amplitude modulates the surface potential at 200°K. A pronounced shift is observed, which goes in the opposite direction for the two groups.

The adjustment procedure of Sec. V produces agreement with the experiment by placing a parabolic edge at 1.42 eV and a saddle-point edge at 2.97 eV.^{16,17} The squares indicate the position of the four resulting peaks, assuming a constant ac field of 15 kV/cm to modulate around different values of the dc bias, as indicated on the right-hand ordinate. The shifts are reproduced correctly as to direction, and the splittings are of the right order of magnitude. No conclusions can be drawn, of course, as to the size of the shifts, since the alignment of the left-hand ordinate with the right-hand ordinate, although probably of the right order of magnitude, is strictly arbitrary. The value of the comparison consists, however, not so much in a numerical agreement as in the possibility for an experimental discrimination among the two different types of transitions, derived from such a calculation and valid for any region of the spectrum.

As long as the character of the surface layer is not known, however, the conclusion is convincing only if a higher edge can be observed in relation to the fundamental edge which serves as a calibration as in the GaAs measurement shown here.

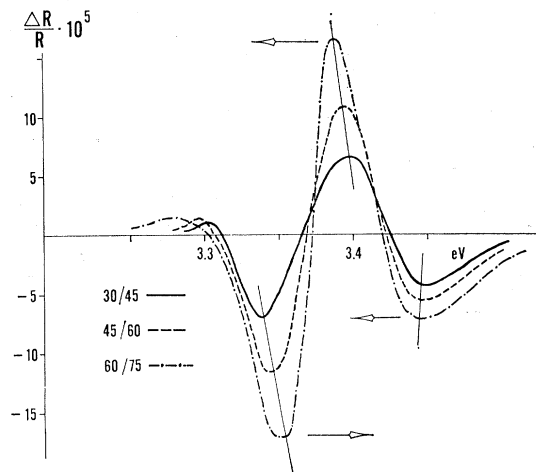


FIG. 12. Reflectance response of the same arrangement of two edges as in Fig. 11, calculated for an ac electric field of 15-kV/cm amplitude, modulating around different values of the dc bias, as indicated. Notice that the saddle-point edge at 3.41-eV shifts opposite to the parabolic edge at 3.33 eV with increasing dc bias.

¹⁶ M. Cardona and G. Harbeke, *J. Appl. Phys.* **34**, 813 (1963).

¹⁷ D. L. Greenaway, *Phys. Rev. Letters* **9**, 97 (1962).

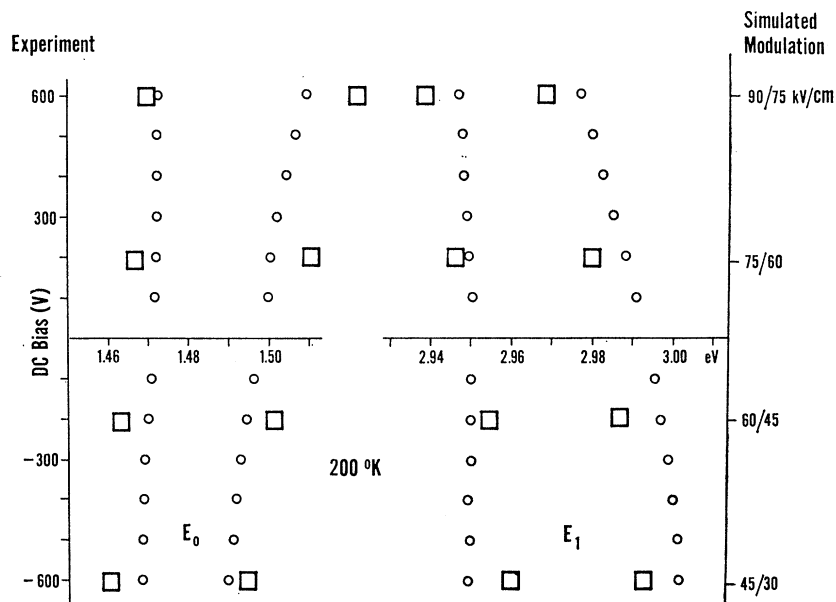


FIG. 13. Shift of the peak positions at a parabolic edge (E_0) and a saddle-point edge (E_1), calculated for a 15-kV/cm modulating field operating around four different values of the dc bias and indicated by squares. Circles give the experimental values in GaAs at 200°K, which correspond qualitatively to this simulated modulation.

VII. CONCLUSIONS

In all spectral regions investigated here, the electroreflectance effect can be understood as a Franz-Keldysh phenomenon, observed in reflection and caused by the electric fields in the surface potential barrier.

The reflectance response at higher interband transitions can be derived from the known response at the fundamental transition, using the Kramers-Kronig dispersion relation and Phillips' duality theorem.

Using reasonable values for lifetime broadening, line shapes of the reflectance response can be calculated, which are distinctly different for different types of interband transitions and in different parts of the spectrum. This facilitates the recognition of basic patterns in the experimentally observed structure. A comparison of the observed and the synthesized structure suggests type and energy of the associated interband transition.

The analysis supports previously reported conclusions about the 3.4-eV region in Si. The experiment is reproduced by the synthesized structure if a parabolic edge is placed at 3.33 eV and a saddle-point edge at 3.41 eV.

Using the transformation properties of the duality theorem and the Kramers-Kronig dispersion relation, it is demonstrated that structure at a saddle-point edge shifts with dc field into a direction opposite to the shift at a parabolic edge. This establishes a valuable experimental criterion, verified for Si and GaAs for the discrimination among the different types of interband transitions.

In order to synthesize the observed reflectance response it is necessary to use the value $\Gamma=0.030 \pm 0.010$ eV for the Lorentzian lifetime-broadening parameter. It is concluded that a study of the electroreflectance effect at various edges and over a range of temperature will yield this lifetime-broadening parameter with considerably higher precision than previous order-of-magnitude determinations.

ACKNOWLEDGMENTS

This study has profited substantially from stimulating discussions with Professor J. C. Phillips, University of Chicago, Professor M. L. Cohen, University of California in Berkeley and with Dr. H. E. Bennett and Dr. V. Rehn of this Laboratory.